

ATMOSPHERIC MONITORING AND RISK ASSESSMENT OF POLYCYCLIC AROMATIC HYDROCARBONS IN A MULTI-INDUSTRIAL CITY

Kwon H-O¹, Lammel G^{2,3}, Jung K-S¹, Choi S-D^{1*}

¹School of Urban and Environmental Engineering, Ulsan National Institute of Science and Technology (UNIST), UNIST-gil 50, Ulsan, 689-798, Republic of Korea; ²Max Planck Institute for Chemistry, Hahn-Meitner-Weg 1, 55128 Mainz, Germany; ³Masaryk University, Research Centre for Toxic Compounds in the Environment, Kamenice 3, 625 00 Brno, Czech Republic

Introduction

Polycyclic aromatic hydrocarbons (PAHs) are composed of two or more fused aromatic rings. They are mainly formed by incomplete combustion from anthropogenic sources (e.g., vehicles and industrial facilities) and natural sources (e.g., volcanos and wildfires). Large amounts of PAHs are directly emitted to the atmosphere and dispersed into the surrounding area and undergo long-range transport to remote areas, including polar regions^{1,2}. Then, they finally accumulate in surface environmental compartments via dry and wet deposition³. PAHs are an important environmental concern because some of them are classified as carcinogenic compounds by the international agency for research on cancer. Residents of urban and industrial areas are often highly exposed to PAHs via inhalation, dermal contact, and ingestion.

The metropolitan city of Ulsan is a representative industrial city in South Korea with petrochemical, automobile, and ship building/heavy industries. Because of these industrial activities and large population (> 1 mn), environmental issues have been a major concern in Ulsan. Industrial complexes are located along the east coast of Ulsan, and residential areas are located close to the industrial complexes. Large amounts of PAHs are expectedly emitted from petrochemical processes and incomplete combustion of fossil fuels^{4,5}.

In this study, we conducted seasonal monitoring of atmospheric PAHs using passive air samplers to investigate the levels, patterns, and spatial distribution of PAHs in Ulsan. These monitoring data were also used for source identification and human health risk assessment. As far as we know, we report the spatially highest resolved data of atmospheric PAHs in urban and industrial areas at least in South Korea.

Materials and methods

Study area and sampling

The Ulsan metropolitan city is located on the south-east coast of the Korean peninsula, and Ulsan is the seventh largest city in South Korea. We seasonally deployed 40 polyurethane foam (PUF) passive air samplers (PAS) in duplicate at 20 sites in Ulsan for one year (spring: February 05–June 10, 2011, summer: June 10–August 25, 2011, fall: August 25–November 18, 2011, and winter: November 18, 2011–February 23, 2012). The sampling sites are classified into three groups: industrial (I1-I6), urban (U1-U10), and rural (R1-R3) sites. PAS address gaseous organic substances, while the particulate phase is almost excluded (by diffusion). The effective PAS sampling volume, needed to convert measured contaminant mass (ng) into atmospheric concentration (ng m⁻³), is dependent on substance properties (K_{oa}), temperature and wind speed and assumed to 3.5 m³ day⁻¹ in agreement with previous observations⁵⁻⁶.

Meteorological and criteria air pollutant (SO₂, CO, NO₂, O₃, and PM₁₀) data were obtained from the websites of the Korea meteorological administration and the Ulsan Institute of Health and Environment (UIHE), respectively.

Instrumental analysis and QA/QC

Target compounds in this study are the 16 US-EPA priority PAHs: naphthalene (Nap), acenaphthylene (Acy), acenaphthene (Ace), fluorene (Flu), phenanthrene (Phe), anthracene (Ant), fluoranthene (Flt), pyrene (Pyr), benzo[a]anthracene (BaA), chrysene (Chr), benzo[k]fluoranthene (BkF), benzo[b]fluoranthene (BbF), benzo[a]pyrene (BaP), indeno[123-cd]pyren (Ind), dibenzo[ah]anthracene (DahA), and benzo[ghi]perylene (BghiP). Among the target compounds, three compounds (Nap, Acy, and Ace) were not considered in this study due to low recoveries and blank contamination. Collected PUF disks were individually Soxhlet extracted for 20 h, and extracts were concentrated by a Turbo Vap. As surrogate standards, deuterated compounds (naphthalene-

d_8 , ace- d_{10} , phe- d_{10} , chr- d_{12} , and perylene- d_{12}) were spiked into the samples prior to extraction. The extract was cleaned up on a silica gel column. As an internal standard, *p*-terphenyl- d_{14} was added to the sample prior to GC injection. PAHs were analyzed by a gas chromatograph-mass spectrometer (GC/MS).

For quality assurance and quality control (QA/QC), every extraction batch of samples included a method blank to check contamination during experiment, and all data were corrected for average blank values. Method detection limits (MDL) were calculated by the multiplication of the standard deviations of seven replicates of the MDL standard and the Student's *t* value (3.14) for a 99% confidence level.

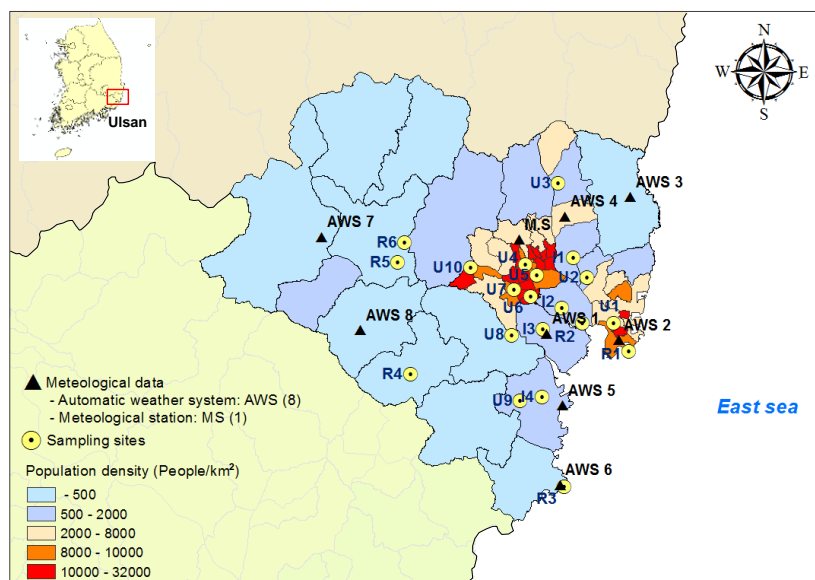


Fig. 1. Location of 20 passive air sampling sites on the population density map of the Ulsan metropolitan city, South Korea.

Source identification and risk assessment

For source identification, we used three methods such as diagnostic ratios, principal component analysis (PCA), and positive matrix factorization (PMF). For human health risk assessment, all the targeted 13 gaseous PAHs were used. The concentrations of individual PAHs were multiplied by Toxic Equivalency Factors (TEFs), and then Toxic Equivalency Quantity (TEQ) values were calculated. PAH exposure was calculated using Monte Carlo simulation. Input parameters were concentration (measured value, triangle distribution), inhalation rate (20 m^3/day , constant), exposure duration (30 years, normal distribution), exposure life (10,500 days, normal distribution), and body weight (70 kg, normal distribution).

Results and discussion

Levels and patterns of PAHs

Among the targeted 13 PAHs, Phe was the most dominant compound, contributing 34% of the total concentration ($\sum_{13}PAHs$) during four seasons, followed by Flt, Pyr, and Flu. This pattern is similar to those reported previously^{1,5}. Fractions of high molecular weight (HMW) PAHs, such as BkF, BaP, Ind, and DahA, were smaller than those of low molecular weight (LMW) PAHs except for Ant. These results indicate that PUF-PAS exclusively collected more volatile/gaseous PAHs. The PAH fraction patterns were different with seasons and sampling sites. Particularly, the fractions of BghiP at industrial sites were higher than those of other HMW PAHs. This could be due to particulate matter containing HMW PAHs collected on PUF disks. The sampling efficiency of PAS for particulate phase organic species is low, but not zero⁶.

The concentration of $\sum_{13}PAHs$ ranged from 13.3 ng/m^3 (spring) to 28.5 ng/m^3 (winter) with an annual mean of 19.8 ng/m^3 . The highest and lowest concentrations of $\sum_{13}PAHs$ were measured in the winter and summer, respectively. Apart from increased domestic fuel consumption (heating) also enhanced long-range atmospheric

transport seemed to have contributed to the highest levels observed in winter. On the other hand, the industrial facilities in Ulsan showed a weak seasonal change in fossil fuel consumption, which suggests that the emissions of PAHs from the industrial complexes are relatively constant throughout the year.

Spatial distribution of PAHs

As expected, the industrial sites showed statistically higher levels of $\sum_{13}\text{PAHs}$ than the urban and rural sites (t -test, $p < 0.05$). However, there was no difference in $\sum_{13}\text{PAHs}$ between the urban and rural sites because some rural sites were close to the industrial complexes, being directly influenced by the industrial emissions.

Seasonal contour plots (Fig. 2) clearly depict the spatial distribution of $\sum_{13}\text{PAHs}$. During all seasons, the industrial sites showed higher levels of PAHs. In particular, two industrial sites (I1 at the automobile industrial complex and I4 at the petrochemical industrial complex) can be considered as hot spots of PAH pollution. In addition, one rural site (R1) also showed higher levels of PAHs because it is nearby the shipbuilding/heavy industrial complex. Overall, the spatial distributions of PAHs look similar across seasons, but the spatial distribution was distinctively affected by seasonal advection patterns (see wind rose diagrams in Fig. 2).

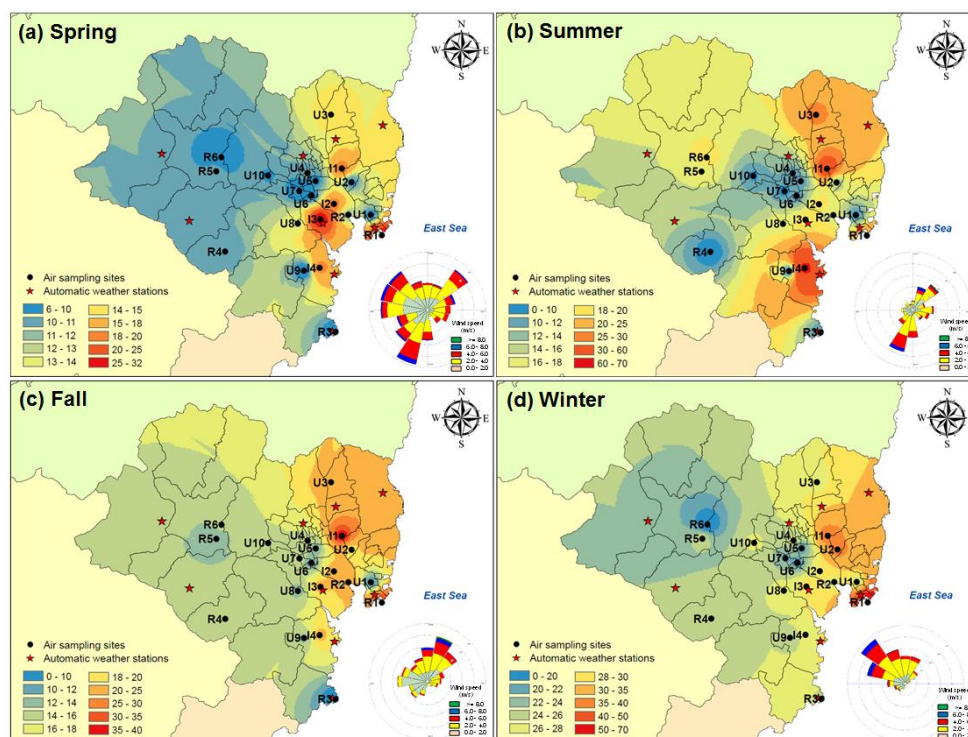


Fig. 2. Spatial distribution of gaseous $\sum_{13}\text{PAHs}$ (ng/m^3) and wind rose diagrams during the four sampling periods. The Inverse Distance Weighted (IDW) interpolation tool from ArcMap 10.1 (Esri's ArcGIS suite) was used for the contour plots.

Source identification

According to the results of PCA, first and second factors accounted for 32% and 54% of the total variance (Fig. 3). By the score plot, two groups were identified from the rural, urban, and industrial sites. Group 1 includes three industrial sites, and Group 2 has all urban and almost rural sites except two rural sites. This result indicates that the urban and rural sites were contaminated by similar PAH sources. Meanwhile, the industrial sites are much more separated from each other, reflecting specific PAH emission patterns from the individual industrial complexes.

As a result of the diagnostic ratios $\text{BaA}/(\text{BaA}+\text{Chr})$, $\text{Flu}/(\text{Flu}+\text{Pyr})$, $\text{Flt}/(\text{Flt}+\text{Pyr})$, $\text{Ind}/(\text{Ind}+\text{BghiP})$ and the PMF model, traffic and industrial facilities were identified as the main sources of PAHs in Ulsan. Particularly, diesel

emission seems to be dominant at all sampling sites, while the industrial sites obviously denoted the specific source effect.

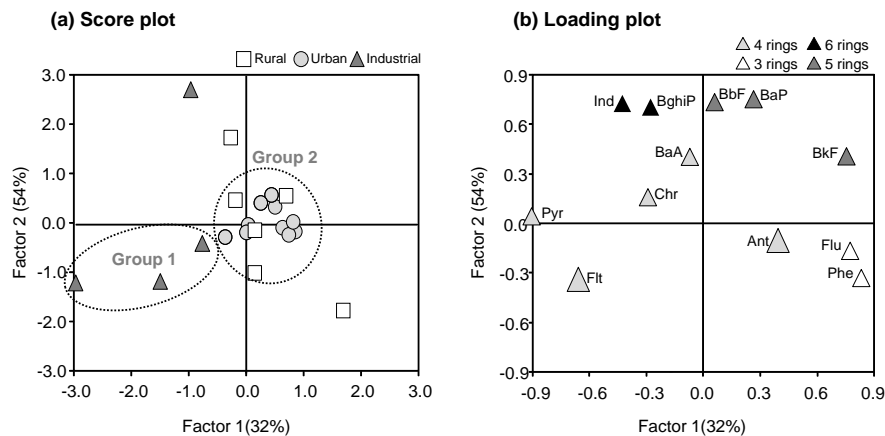


Fig. 3. Results of principal components analysis for annual PAH patterns at 20 sites in Ulsan, South Korea.

Human health risk assessment

The human health risk by 13 gaseous PAHs ranged seasonally as follows: 2.8×10^{-8} – 3.9×10^{-7} in the spring, 3.7×10^{-8} – 2.1×10^{-7} in the summer, 3.9×10^{-8} – 3.2×10^{-7} in the fall, and 4.8×10^{-8} – 4.2×10^{-7} in the winter. As expected, the risk at the industrial sites in the winter was the highest. These levels of risk of gaseous PAHs were lower than the US-EPA safety level of PAHs ranging from 1.0×10^{-4} to 1.0×10^{-6} .

In general, less volatile PAHs are more toxic, and they are mostly associated with particulate matter. Therefore, the calculated risk using (mostly) gaseous PAH would underestimate the actual risk from PAH in ambient air. To overcome this problem, we estimated particulate PAH concentrations using a dual (adsorption + absorption) gas-particle partitioning model (GPPM)⁷, which performs best among various GPPMs in use⁸⁻¹⁰. The combined risk by gaseous and particulate PAHs was exceeding the US-EPA safety level.

Acknowledgements

This work was supported by a Ulsan National Institute of Science and Technology (UNIST) grant funded in 2013.

References:

1. Choi SD, Ghim YS, Lee JY, Kim JY, Kim YP. (2012); *J Hazard Mater.* 227–228: 79–87
2. Choi SD, Shunthirasingham C, Daly GL, Xiao H, Lei YD, Wania F. (2009); *Environ poll.* 157: 3199–3206
3. Lee BK, Lee CB. (2004); *Atmos Environ.* 38(6): 863–871
4. Ma WL, Li YF, Qi H, Sun DZ, Liu LY, Wang DG. (2010); *Chemosphere.* 79: 441–7
5. Choi SD, Kwon HO, Lee YS, Park EJ, Oh JY. (2012); *J Hazard Mater.* 241–242: 252–258
6. Klánová J, Cupr P, Kohoutek J, Harner T. (2008); *Environ Sci Technol* 42: 550–555
7. Lohmann R, Lammel G. (2004); *Environ Sci Technol* 38: 3793–3803
8. He J, Balasubramanian R. (2009); *Atmos Environ* 38: 4375–4383
9. Lammel G, Sehili AM, Bond TC, Feichter J, Grassl H. (2009); *Chemosphere* 76:98–106
10. Landlová L, Čupr P, Franců J, Klánová J, Lammel G. (2014); *Environ. Sci. Pollut. Res.* 21 : 6188–6204